



HAL
open science

Displacement of η^5 -cyclopentadienyl ligands from half-sandwich C,C-(NHC-cyanoalkyl)–nickel(II) metallacycles: further insight into the structure of the resulting Cp-free nickelacycles and a catalytic activity study

Bernardo de Pina Cardoso, Jean-Marie Bernard-Schaaf, Saurabh Shahane, L Veiros, Michael Chetcuti, Vincent Ritleng

► To cite this version:

Bernardo de Pina Cardoso, Jean-Marie Bernard-Schaaf, Saurabh Shahane, L Veiros, Michael Chetcuti, et al.. Displacement of η^5 -cyclopentadienyl ligands from half-sandwich C,C-(NHC-cyanoalkyl)–nickel(II) metallacycles: further insight into the structure of the resulting Cp-free nickelacycles and a catalytic activity study. Dalton Transactions, 2018, 47, pp.1535-1547. 10.1039/C7DT04560C . hal-02166522

HAL Id: hal-02166522

<https://hal.science/hal-02166522>

Submitted on 14 Dec 2021

HAL is a multi-disciplinary open access archive for the deposit and dissemination of scientific research documents, whether they are published or not. The documents may come from teaching and research institutions in France or abroad, or from public or private research centers.

L'archive ouverte pluridisciplinaire **HAL**, est destinée au dépôt et à la diffusion de documents scientifiques de niveau recherche, publiés ou non, émanant des établissements d'enseignement et de recherche français ou étrangers, des laboratoires publics ou privés.

Displacement of η^5 -cyclopentadienyl ligands from half-sandwich *C,C*-(NHC-cyanoalkyl)–nickel(II) metallacycles: further insight into the structure of the resulting Cp-free nickelacycles and a catalytic activity study

Received 00th January 20xx,
Accepted 00th January 20xx

DOI: 10.1039/x0xx00000x

www.rsc.org/

Bernardo de P. Cardoso,^a Jean-Marie Bernard-Schaaf,^a Saurabh Shahane,^a Luis F. Veiros,^b Michael J. Chetcuti*^a and Vincent Ritleng*^{a,c}

The four cationic *C,C*-(NHC-cyanoalkyl)–nickel(II) metallacyclic complexes, [Ni{Me-NHC-CH₂CH(CN)}(NCMe)](PF₆) (**2a**), [Ni{Mes-NHC-CH₂CH(CN)}(NCMe)](PF₆) (**2b**), [Ni{Mes-NHC-(CH₂)₂CH(CN)}(NCMe)](PF₆) (**2c**) and [Ni{DiPP-NHC-(CH₂)₂CH(CN)}(NCMe)](PF₆) (**2d**) were prepared by the removal of the Cp ligand under acidic conditions at 0 °C from the corresponding half-sandwich nickelacycles [NiCp{R-NHC-(CH₂)_nCH(CN)}] (**1a–1d**; Cp = η^5 -C₅H₅; n = 1 or 2; R-NHC-(CH₂)_nCH(CN) = 1-R-3-[(CH₂)_nCH(CN)]-imidazol-2-ylidene). Full characterization of **2a–d** by ¹H and ¹³C{¹H} NMR spectroscopy in CD₃CN and pyridine-*d*₅, ATR-FTIR spectroscopy, mass spectrometry, and CHN microanalyses established the presence of *only one acetonitrile ligand per nickel atom* in the solid state. A DFT structural study conducted on the cations of the methyl-substituted 5-membered nickelacycle **2a** and the mesityl-substituted 6-membered cycle **2c** found a small energetic cost ($\Delta G = 7\text{--}12 \text{ kcal.mol}^{-1}$) for the loss of one acetonitrile ligand from the square-planar structures existing in solution, that should be easily amenable upon solvent evaporation ($\Delta G^\ddagger = 14 \text{ kcal.mol}^{-1}$ in the case of **2c**). Two structures with one acetonitrile ligand could be optimized in both cases: (i) a truly T-shaped 14-electron structure with an end-on acetonitrile ligand, and (ii) a masked T-shaped structure stabilized by the π -coordination of the dangling CN group of the metallated alkyl chain, the latter being favoured by 2.4 kcal.mol⁻¹ in the case of the flexible 6-membered ring **2c**. Comparison of calculated vibrational frequencies with experimental FTIR spectra ruled out π -coordination of the dangling CN group as a $\nu(\text{C}\equiv\text{N})$ band at low frequency was absent. Complexes **2a–d** thus probably exist as rare three-coordinate T-shaped 14-electron species in the solid state. Their catalytic activity was studied for the direct arylation of azoles, and **2c** proved to be moderately active for the coupling of benzothiazole with aryl iodides. Mechanistic insights suggest that competing processes or a radical process catalysed by nickel particles could follow an initial reduction of **2c** by the dimerization of a sacrificial amount of benzothiazole.

Introduction

Coordinatively and electronically unsaturated complexes are often proposed as key intermediates in transition metal-catalyzed reactions. Thus, ligand dissociation to form intermediates with open coordination sites is frequently postulated as the initial step in reactions involving 16-electron square-planar precatalysts. Resulting T-shaped d⁸ three-coordinate complexes remain however a curiosity and well-characterized examples are rare.¹ In particular, only a handful of truly T-shaped 14-electron nickel(II) species – where no stabilizing secondary interaction (agostic bond, solvent molecule or counteranion) is observed at the fourth position of

the square plane – have been described.² In all but one case,^{2a} these species bear a bulky 1,3-(2,6-diisopropylphenyl)imidazol-2-ylidene (IPr) or tricyclohexylphosphine (PCy₃) ligand and are comprised of a mono- or di-anionic *C,N*- or *C,O*-nickelacycle (Scheme 1). Herein we report a series of cationic nickelacycles bearing a mono-anionic *C,C*-NHC-cyanoalkyl chelate, for which elemental analyses, NMR, HRMS, and FTIR spectra, coupled to DFT calculations suggest they exist as 14-electron T-shaped three-coordinate species in the solid state.

We recently reported the facile and clean removal of the η^5 -cyclopentadienyl (Cp) ligand from 18-electron half-sandwich nickelacycles **1** bearing an anionic NHC-cyanoalkyl tether under acidic conditions in acetonitrile.³ Neutral 16-electron square-planar complexes **3** were isolated and fully characterized after treatment of the resulting cationic species **2**, bearing labile acetonitrile ligand(s) with potassium acetyl-

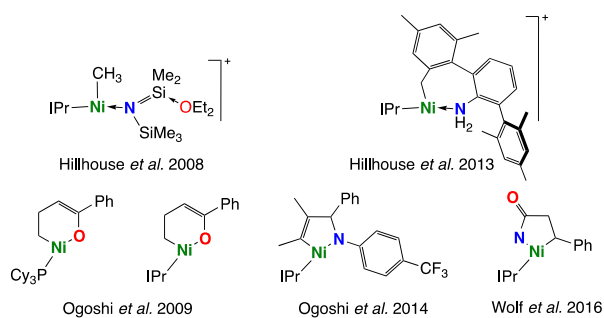
^a Université de Strasbourg, Ecole européenne de Chimie, Polymères et Matériaux, CNRS, LCM UMR 7509, F-67000 Strasbourg, France. E-mails:

michael.chetcuti@unistra.fr, ritleng@unistra.fr

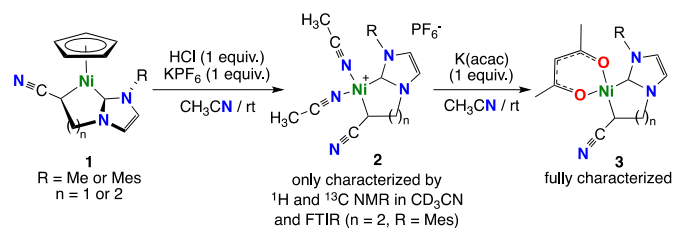
^b Centro de Química Estrutural, Complexo I, Instituto Superior Técnico, Av. Rovisco Pais, 1049-001 Lisboa, Portugal.

^c Institut Universitaire de France, F-75000 Paris, France

Electronic Supplementary Information (ESI) available: synthetic details, ¹H and ¹³C NMR spectra, FTIR spectra, crystallographic information and atomic coordinates of the optimized species. CCDC 1585953 and 1585956. For ESI and crystallographic data in CIF or other electronic format, see DOI: 10.1039/x0xx00000x



Scheme 1 Well-characterized T-shaped tricoordinate nickel(II) complexes.²



Scheme 2 Cp acidolysis in acetonitrile (**1** to **2**) and subsequent complexation by an acetylacetonate chelate (**2** to **3**). Proposed square-planar structure of complexes **2**.³

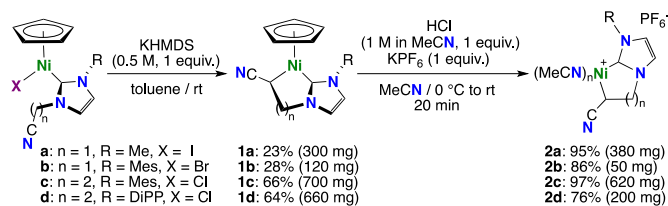
acetate (Scheme 2). Remarkably, the nickel–alkyl and nickel–carbene bonds were not ruptured in this unprecedented Cp acidolysis. This robustness opened up interesting perspectives for the use of the potentially unsaturated Cp-free cationic species **2**. The latter, however, proved difficult to recrystallize and were ill-characterized.³ Further work on their characterization was therefore needed prior to studying their reactivity. Our findings, which show they are not square-planar with two acetonitrile ligands in the solid state as initially presumed (Scheme 2), are described herein. Their activity as precatalysts for the arylation of azoles is also reported.

Results and discussion

Synthesis and characterization of a series of cationic species (**2**)

A series of four species **2** (**2a**: n = 1, R = Me; **2b**: n = 1, R = Mes; **2c**: n = 2, R = Mes; **2d**: n = 2; R = DiPP, where Mes = mesityl and DiPP = 2,6-diisopropylphenyl) were prepared *via* optimized synthetic routes (Scheme 3).

Treatment of the half-sandwich [Ni(NHC)XCp]⁴ complexes (**a-d**) bearing an alkylnitrile side arm with potassium bis(trimethylsilyl)amide (KHMDs) in toluene at room temperature allowed the abstraction of one of the methylene hydrogen atoms in the α position to the nitrile group. Use of KHMDs instead of KOtBu, as previously reported,^{5,6} was found to give cleaner reactions and the half-sandwich nickelacycles **1a-d** were isolated in yields varying from *ca.* 25 % for the 5-membered cycles to *ca.* 65 % for the 6-membered cycles on multi-hundred mg scales (Scheme 3). The novel complexes **1b** and **1d** were fully characterized by ¹H and ¹³C{¹H} NMR and IR



Scheme 3 Optimized syntheses of the nickelacycles **1a-d** and **2a-d**.

spectroscopy and by CHN microanalyses. Their spectroscopic features are similar to those of the previously reported species **1a** and **1c** and deserve no particular comment (see Fig. S1 to S8, ESI).

X-ray quality crystals of **1a** and **1b** were grown from concentrated solutions in THF and their structures were established by X-ray diffraction studies. Crystallographic data and data collection and refinement parameters are grouped together in Table S1 (see ESI). The structures of **1a** and **1b** are depicted in Figure 1 and 2, respectively, and key bond lengths and bond angles are collected in the figure captions. Both complexes have structures that are closely related to each other, with slightly puckered nickelacyclic rings, and to that of **1c** that was reported earlier.⁵ The only notable difference resides in the C_{NHC}–Ni–C_{alkyl} bite angle that is considerably narrower in the 5-membered metallacycles **1a** and **1b** (*ca.* 84.7°) than in the 6-membered metallacycle **1c** (93.9°),⁵ which may explain the lower yields observed for the formation of the 5-membered cycles.

Removal of the Cp ligand of **1a-d** was then achieved by reaction with equimolar amounts of HCl (1 M) and KPF₆ in acetonitrile. Adding HCl at 0 °C instead of room temperature was found to give even cleaner reactions than reported for **2c** (Scheme 2),³ and the nickelacycles **2a-d** were obtained in good to excellent isolated yields[†] after thorough drying under high vacuum of the resulting moderately air-stable dark yellow powders (Scheme 3).

Nickelacycles **2a-d** are very poorly soluble or insoluble in most common solvents such as toluene, benzene, *n*-pentane,

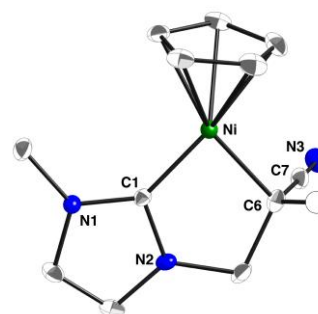


Figure 1 Molecular structure of **1a**. The only hydrogen atom shown is that of the CHCN group (as a white isotropic sphere). Ellipsoids are shown at the 50% probability level, and key atoms are labelled. The centrosymmetric space group *P2₁/c* contains both enantiomers; only the (*S*) enantiomer is shown. Selected distances (Å) and angles (°) with esds's in parenthesis: Ni–C1, 1.8475(11); Ni–C6, 1.9697(11); C6–C7, 1.4491(17); C7–N3, 1.1491(17); Ni–Cp_{cent}, 1.756; C1–Ni–C6, 84.71(5); C1–Ni–Cp_{cent}, 140.9; C6–Ni–Cp_{cent}, 134.3; C6–C7–N3, 178.84(14).

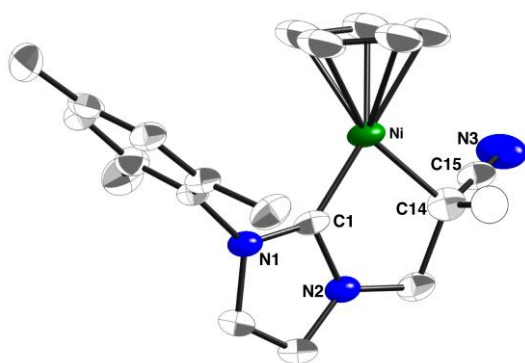


Figure 2 Molecular structure of **1b**. The only hydrogen atom shown is that of the CHCN group (as a white isotropic sphere). Ellipsoids are shown at the 50% probability level, and key atoms are labelled. Two independent but very similar molecules (A and B) are present in the asymmetric unit. The centrosymmetric space group $P-1$ contains both enantiomers of each molecule and only the (*S*) enantiomer of molecule A is shown. Selected distances (Å) and angles (°) with esd's in parenthesis of the two independent molecules are given here: Ni–C1, 1.842(6), 1.844(5); Ni–C14, 1.980(7), 1.969(6); C14–C15, 1.432(9), 1.444(9); C15–N3, 1.135(8), 1.142(8); Ni–Cp_{cent}, 1.748, 1.754; C1–Ni–C14, 85.2(3), 84.3(2); C1–Ni–Cp_{cent}, 141.8; 142.9 C14–Ni–Cp_{cent}, 132.8, 132.7; C14–C15–N3, 177.8(8), 179.0(7).

chloroform, diethyl ether, tetrahydrofuran, 1,4-dioxane or water, readily decompose in halogenated solvents such as dichloromethane and tetrachloroethane, and are *extremely* soluble in polar coordinating solvents such as acetone, dimethylsulfoxide, methanol, nitromethane, acetonitrile or pyridine – the latter two being the only ones in which they are soluble and stable. Despite repeated attempts, none of them could be recrystallized and no X-ray quality crystals could be grown. Crystals of $[\text{Ni}(\text{CH}_3\text{CN})_6](\text{PF}_6)_2$, resulting from the decomposition of **2c** in acetonitrile, were harvested twice.

Nickelacycles **2a–d** were thus characterized by ^1H and $^{13}\text{C}\{^1\text{H}\}$ NMR spectroscopy in CD_3CN and pyridine- d_5 , ATR-FTIR spectroscopy, mass spectrometry, and by CHN microanalyses. Similarly to what had been observed for **2c**,³ the ^1H and ^{13}C NMR spectra of **2a,b,d** in CD_3CN clearly show the presence of the metallacycles, whose signals' chemical shifts and multiplicities are similar to those of their precursors **1a,b,d** (see Fig. S9 to S24, ESI). Interestingly, the ^1H NMR spectra of **2b** and **2c** display two singlets in a 1:1 integrated ratio for the two *meta*-hydrogen atoms as well as two singlets in a 3:3 relative integrated ratio for the *ortho*-methyl groups of the mesityl substituents, both of which suggest restricted rotation about the N–mesityl bond on the NMR time scale. Similarly, two doublets (for the *meta* aromatic ring protons), two septets (for the CH protons of the isopropyl groups), and four doublets (for the methyl protons of the isopropyl groups) are observed in the ^1H NMR spectrum of **2d**, all of which indicate restricted rotation about the N–DiPP (2,6-diisopropylphenyl) bond as well. Furthermore, the ^{13}C NMR spectra of **2a–d** all display relatively broad signals for the carbons that are bound to the nickel centre, *i.e.*: for the carbene and CHCN carbons. This may result from a fluxional process related to the lability of the acetonitrile ligands (*vide infra*).⁵ In addition, it is worth mentioning that the carbene carbon signals of **2a–d** are all high field shifted (153.8–158.4 ppm in CD_3CN) when compared to **1a–d** (171.3–175.9 ppm)^{5,6a} and **3a** (163.1 ppm)³, which likely

indicates an increase in Lewis acid character of the nickel centre caused by a decrease in the σ -donor ability of the ancillary ligands ($\text{NCMe} < \text{acac}^- < \text{Cp}^-$).⁷

Regarding the acetonitrile ligands, the presence in the ^1H NMR (CD_3CN) spectra of **2a–d** of a singlet on the downfield side of the solvent residual multiplet (at 1.96 ppm) indicates the presence of free CH_3CN resulting from $\text{CH}_3\text{CN}–\text{CD}_3\text{CN}$ exchange. Integration of this singlet systematically indicated the presence of three protons relatively to the other signals (Fig. S9, S13, S17 and S21), which suggested the presence of only one acetonitrile molecule per “naked” nickelacycle in the solid state. Similarly, the ^1H NMR spectra of **2a–d** in pyridine- d_5 (see Fig. S10, S14, S18 and S22) all display one singlet integrating for three protons (relative to the metallacycles' signals) at 1.83–1.86 ppm, which shows the presence of one acetonitrile molecule per “naked” nickelacycle. Interestingly in all cases but **2a**, the acetonitrile molecule is observed as free acetonitrile, as pyridine- d_5 has probably displaced the labile acetonitrile ligand. In contrast for **2a**, the chemical shifts of the acetonitrile molecule (see Fig. S10 and S12) indicate that it is coordinated to the nickel atom, and suggest that in this case pyridine- d_5 associates as a fourth ligand but does not displace the MeCN ligand.

In agreement with the NMR data, HRMS spectra of **2a–d** (MeCN solution, electrospray ionization, positive ion mode) all show the $[\text{nickelacycle}–\text{NCMe}]^+$ ion as the base peak, and elemental analyses also confirmed the formulation with *only one acetonitrile ligand per nickel atom*. All this excludes the possibility of complexes **2** being 16-electron square-planar species with two acetonitrile ligands in the solid state, as initially presumed.³ The suspected fluxional behaviour observed in solution (*vide supra*) may hence originate from an equilibrium between the saturated square-planar and an unsaturated species.

Regarding the nature of this formally unsaturated species, several hypotheses may be drawn. Complexes **2** may *a priori* exist as: (i) dimers and/or oligomers with bridging acetonitrile ligands as postulated after similar loss of an acetonitrile ligand upon drying under vacuum for a related (but with bridging bromide ligands) C,C-NHC,cycloheptatrienyl-palladacycle,⁸ (ii) monomers containing very rare examples of four-electron donor side-on acetonitrile ligand,⁹ or (iii) rare three-coordinate 14-electron Ni(II) species with an end-on acetonitrile ligand.²

In the former case, the possible existence of dimers and/or oligomers in equilibrium with the more likely square-planar species in solution could explain why crystals of complexes **2a–d** could not be grown.^{8,10} However, bridging acetonitrile ligands are rare,^{11,12,13,14} and we are aware of only one structurally characterized example with a metal of groups 8–10: a tetranuclear nickel complex, $[\text{Ni}(\text{PCy}_3)(\text{NCMe})]_4$,¹⁵ in which μ_2, η^1, η^2 -acetonitrile ligands¹⁶ are π -bonded to a nickel centre and σ -bonded to a second one. Four-electron side-on acetonitrile ligands are even more rare and have only been described with group 6 metals.^{9,17} In addition, in both cases, the $\text{C}\equiv\text{N}$ stretch of the acetonitrile ligands should appear around 1700 cm^{-1} ,^{9d,e,15,17} which is not the case here (see Fig. S25 to S28, ESI) and militates against these hypotheses.

However, it is well known that $\nu(\text{C}\equiv\text{N})$ bands may be weak^{9d,e,12c,f} or sometimes unobserved.^{9a,b,c,18} Hence, the absence of a significant band between 1600 and 1800 cm^{-1} in the IR spectra of **2a-d** (Fig. S25 – S28) should not be considered definitive, and these hypotheses cannot be totally ruled out on this sole basis.

In the case of rare but known three-coordinate 14-electron Ni(II) species,² much more frequent end-on acetonitrile ligands should be present and the acetonitrile $\text{C}\equiv\text{N}$ stretch would be expected to appear between 2200 and 2300 cm^{-1} .¹⁹ This in agreement with the medium intensity peaks observed between 2233 and 2243 cm^{-1} in the spectra of **2a-d** (Fig. S25 – S28). However, the $\text{C}\equiv\text{N}$ stretch of the cyanoalkyl arm is expected in the same area, and although the observed bands show a shoulder at *ca.* 2195–2200 cm^{-1} and may thus be the result of an overlap of these two vibrations, we cannot ascribe them with certainty at this stage.

Density functional theory (DFT) structural study of complexes (**2**)

To try to solve these issues and get further insight to the structure of complexes **2**, we undertook a DFT structural study on the cations of both the methyl-substituted 5-membered nickelacycle **2a** and the mesityl-substituted 6-membered cycle **2c**. Calculation of the free energy balance of the species with one and two end-on acetonitrile ligands allowed us to identify three stable structures in each case: (i) the 16-electron square-planar structure, (ii) a truly T-shaped 14-electron structure, and (iii) a T-shaped structure with the dangling CN group of the metallated alkyl chain π -coordinated to the nickel centre (Fig. 3). Three-coordinate Y-shaped species were found unstable, which is consistent with the fact that complexes **2** are diamagnetic,²⁰ in solution and in the solid state.^{55, 555}

In the case of the 6-membered ring **2c**, the cation with only one acetonitrile ligand would be stabilized by π -coordination of the dangling CN group by 2.4 $\text{kcal}\cdot\text{mol}^{-1}$. However, this isomer, **2c-NCMe-CN⁺**, is still about 7.1 $\text{kcal}\cdot\text{mol}^{-1}$ higher in energy than the species with two coordinated acetonitrile ligands, **2c-(NCMe)₂⁺** (Fig. 3-right). The formation of the latter from **2c-NCMe-CN⁺** starts from the pair of reagents, **Int** (Fig. 4), that is 6 $\text{kcal}\cdot\text{mol}^{-1}$ less stable than the separated reagents and has a 4.76 Å distance between the Ni centre and the N atom of the incoming acetonitrile. The following transition state (**TS1**) is a rather early one with a large Ni–N distance (3.80 Å) and a negligible energy barrier ($\Delta G^\ddagger = 1 \text{ kcal}\cdot\text{mol}^{-1}$). Overall, the reaction is exergonic with a free energy balance of $\Delta G = -7 \text{ kcal}\cdot\text{mol}^{-1}$ (Fig. 4).

Importantly, a π -bound nitrile isomer of **2c-NCMe⁺** could not be optimized. It is not stable and spontaneously yields **2c-NCMe⁺**, which allows us to rule out this hypothesis. In addition, the most stable dimer that could be optimized, (**2c-NCMe₂**)₂²⁺, shows one “naked” nickelacycle and one nickelacycle bearing an end-on acetonitrile, linked together by a μ_2 - η^1, η^1 -bridging acetonitrile ligand (Scheme 4). However, dimerization is an unfavourable process with a free energy balance of +11 $\text{kcal}\cdot\text{mol}^{-1}$, and thus is not expected.

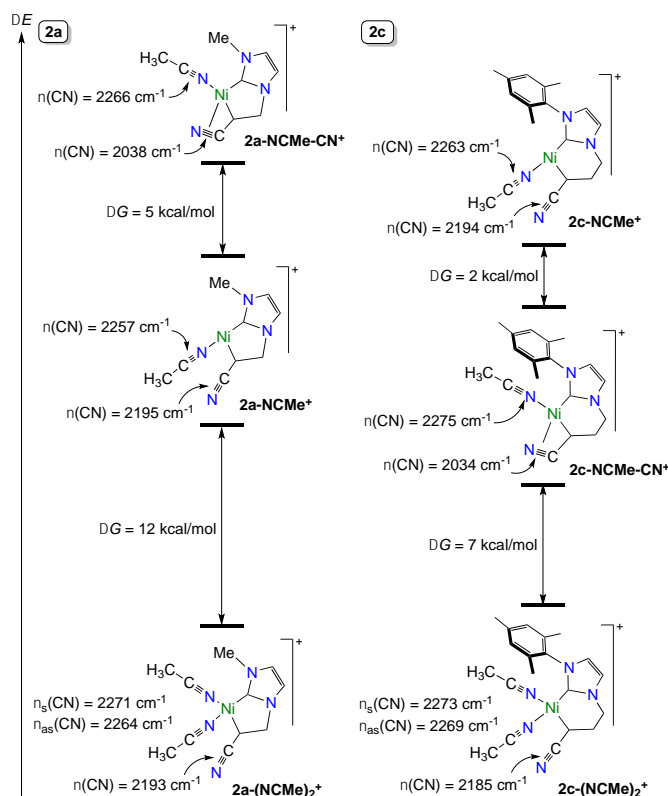


Figure 3 Free energy balances of the structures of **2a** and **2c** cations with one or two end-on acetonitrile ligands, and calculated vibrational frequencies of the $\text{C}\equiv\text{N}$ bonds.

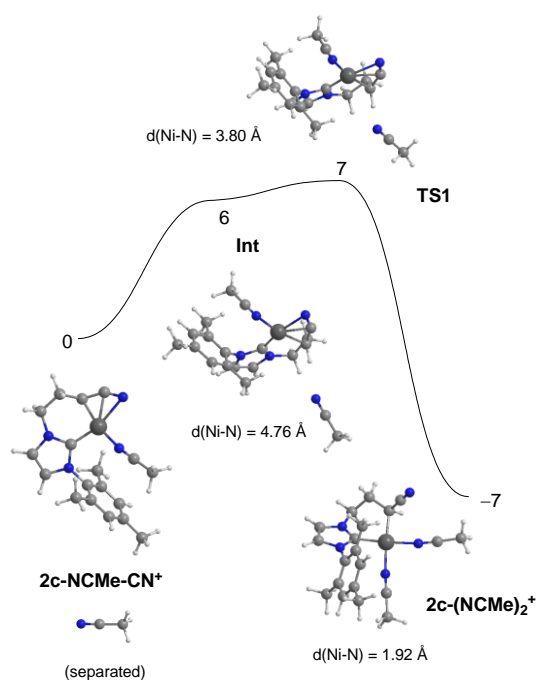
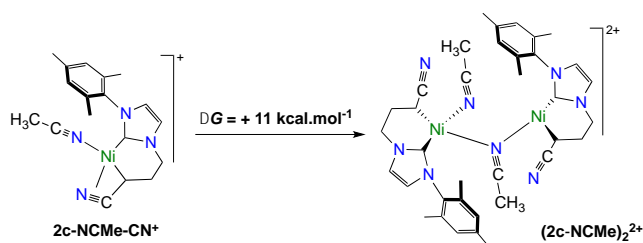


Figure 4 Free energy profile and optimized structures of the relevant species for the coordination of a second acetonitrile molecule to **2c-NCMe-Me⁺**. Free energy values (kcal·mol⁻¹) relative to the separated reactants.

Scheme 4 Free energy balance of the dimerization of **2c-NCMe-CN**⁺

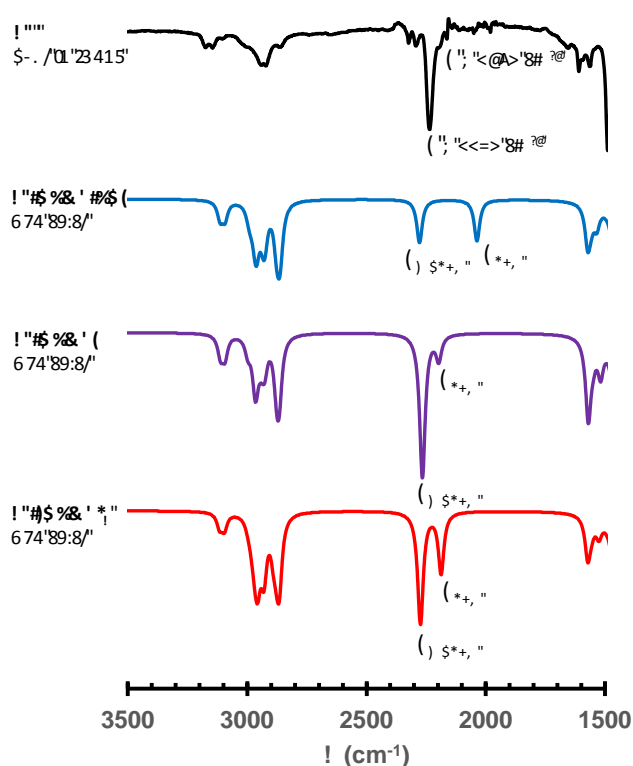
In the case of the more strained 5-membered nickelacycle **2a**, the free energy balance of the cation bearing only one acetonitrile ligand suggests that the dangling CN group is not coordinated to the nickel atom; the coordinated isomer, **2a-NCMe-CN**⁺, being 5 kcal.mol⁻¹ higher in energy than the T-shaped species, **2a-NCMe**⁺. The latter is 12 kcal.mol⁻¹ less stable than the square planar species **2a-(NCMe)₂**⁺ (Fig. 2-left).

In summary, these DFT calculations demonstrate that although the square planar isomers are more stable by 7 to 12 kcal.mol⁻¹, loss of one of the two acetonitrile molecules present in the dissolved species could be easily obtained upon crystallization (energy barrier of only 14 kcal.mol⁻¹ in the case of **2c**), especially if the latter occurs *via* solvent evaporation, which is the case here. Interestingly, the exact structure of the resulting monomeric species bearing one end-on bound acetonitrile ligand would depend on the ring size of the nickelacycle, the dangling CN group of the metallated alkyl chain being π -coordinated to the nickel centre in the case of flexible 6-membered cycles. If that were to occur, the IR signature of the 5-membered species, **2a** and **2b**, should be different from those of the 6-membered species, **2c** and **2d** (Fig. 3). The IR spectra of **2a-d** are however remarkably similar (see Fig. S27–S30). Moreover, none of them shows a band in the 2020–2030 cm⁻¹ range that would correspond to the π -bound CN group of the metallated alkyl chain, and the experimental spectra of **2c** closely resemble the DFT-simulated spectra of **2c-NCMe**⁺ (Fig. 5). Hence, the complexes **2a-d** most probably exist as truly T-shaped 14-electron species in the solid state.^{§§§§}

Catalytic study of complexes (**2**)

Over the last 10 years, nickel complexes have emerged as very promising catalysts for C–H bond functionalization reactions.²¹ In particular, nickel-catalysed biaryl couplings between (hetero)arenes and aryl halides,²² phenol derivatives,²³ or aryl esters²⁴ have been demonstrated to be reliable alternatives to palladium-catalysed cross-couplings. It is noteworthy that in nearly all reported examples, a Ni(0) or Ni(II) source is associated to a neutral *N,N*-^{22a,b,d} or *P,P*-^{23,24} bidentate ligand. Thus, the isolation and characterization of complexes **2** opened up the possibility of observing how a robust anionic *C,C*-chelate comprising a NHC moiety would behave in such couplings.

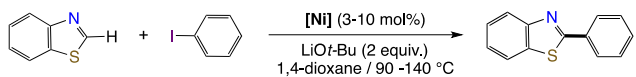
Initial studies focused on the coupling of benzothiazole with iodobenzene catalysed by **2c** under conditions akin to those established by Itami *et al.* for their Ni(OAc)₂/bipyridine

Figure 5 IR (ATR) spectrum of **2c** and DFT-simulated spectra of **2c-NCMe-CN**⁺, **2c-NCMe**⁺ and **2c-(NCMe)₂**⁺.

system,^{22a,d} but with only 5 mol% of nickel instead of 10 mol%, *i.e.*: in 1,4-dioxane at 90–140 °C in the presence of **2c** (5 mol%) and LiOtBu (2 equiv.). At 90 °C, no reaction was observed after 16 h (Table 1, entry 1). Increasing the temperature to 140 °C afforded an encouraging 51 % conversion after 16 h reaction (entry 2). The conversion, however, dropped to 26 % when the catalyst loading was reduced to 3 mol%, and did not increase significantly when it was increased to 10 mol% (entries 3 and 4). No conversion was observed in the absence of LiOtBu (entry 5) or in the presence of any other base, including the sodium and potassium analogues of LiOtBu (Table S2, ESI), demonstrating that the choice of the base is crucial as has often been reported.^{22–24} The choice of the solvent also proved crucial as little or no conversion was observed in any other solvent (Table S2). Satisfyingly, significant improvements of the conversion to 69 and 78 % were observed after 18 and 36 h of reaction, respectively (entries 6 and 7).

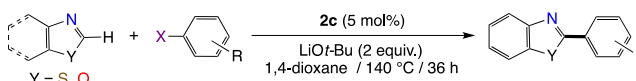
The activities of complexes **2a-d** were then compared using the conditions of entry 2 or 6. An equivalent conversion was obtained with the mesityl-substituted 5-membered nickelacycle **2a** (66 %, Table 1, entry 8), showing that the ring size has almost no influence on the catalytic activity. In contrast, the methyl-substituted 5-membered cycle **2b** and the DiPP-substituted 6-membered ring **2d** gave lower conversions of 57 and 8 % (entries 9 and 10), showing the importance of the steric footprint of the NHC moiety.

Finally, the activities of the half-sandwich precursor, **1c**, and of the square-planar derivative, **3c**, of **2c** were evaluated

Table 1 Optimization of the coupling of benzothiazole with iodobenzene^a


Entry	Catalyst (mol%)	Temperature (°C)	Time (h)	Conv. (%) ^b
1	2c (5)	90	16	0
2	2c (5)	140	16	51
3	2c (3)	140	16	26
4	2c (10)	140	16	56
5 ^c	2c (5)	140	16	0
6	2c (5)	140	18	69
7	2c (5)	140	36	78
8	2a (5)	140	18	66
9	2b (5)	140	18	57
10	2d (5)	140	16	8
11	1c (5)	140	16	0
12	3c (5)	140	16	24

^a Reaction conditions: benzothiazole (1 equiv.), iodobenzene (1.5 equiv.), LiOtBu (2 equiv.), **1c**, **2a-d** or **3c** (3-10 mol%) in 1,4-dioxane at 90-140 °C for 16-36 h. ^b Conversion determined by GC; average value of two runs. ^c No LiOtBu.

Table 2 Arylation of azoles with haloarenes catalysed by **2c**^a


Entry	Azole	Aryl halide	X, Y	Conv. (%) ^b	Yield (%) ^c
1			X = I	78	43
2			X = Br	0	-
3			X = I	56	47
4			X = Cl	0	-
5				35	25
6				-	14
7				49	45
8				68	59
9				-	13
10				-	17
11			Y = S	-	n.d. ^d
12			Y = O	-	-
13				-	11

^a Reaction conditions: azole (1 equiv.), aryl halide (1.5 equiv.), LiOtBu (2 equiv.), **2c** (5 mol%) in 1,4-dioxane at 140 °C for 36 h. ^b Conversion to the desired coupling product determined by GC; average value of two runs. ^c Isolated yields; average value of two runs. ^d A complex isomeric mixture was obtained.

under the conditions of entry 2. No conversion was observed with **1c** and only 24 % with **3c**, showing that labile ligands and/or an unsaturated nickel centre are required to observe a satisfactory activity.

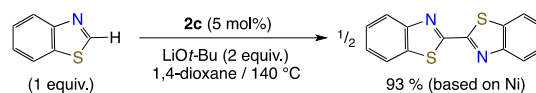
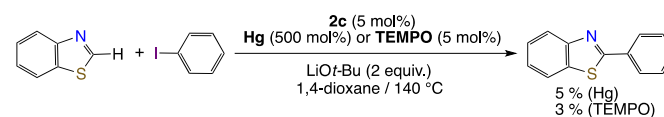
With the optimized conditions in hand (Table 1, entry 7), we then briefly examined the scope of the heteroarene arylation reaction with **2c** (Table 2). Benzothiazole was arylated with moderate to good yields with iodobenzene, 4-

iodotoluene, and the electron-poor 4-iodobenzonitrile and 4-iodobenzotrifluoride (entries 1, 3, 7 and 8). However, it does not react with bromo- or chloro-arenes (entries 2 and 4). The electron-rich 4-iodoanisole, and the sterically encumbered 2-iodo-toluene gave rather low yields (entries 5 and 9). On the other hand, iodobenzene gave only poor yields with other azoles, such as 4,5-dimethylthiazole and 5-phenyloxazole (entries 10 and 13), and complex mixtures of isomers were obtained with oxazole and thiazole (entries 11 and 12) due to selectivity issues. All in all, **2c** is thus a moderately active catalyst for the arylation of benzothiazole with aryl iodides.

Regarding the reaction mechanism, it is significant that a small amount (< 5% based on the maximum possible amount of the coupling product) of the dimerization product of benzothiazole was systematically observed. This may suggest initial reduction of **2c** to an active species by nickelation of two molar equivalents of deprotonated benzothiazole followed by reductive elimination, as was proposed by Itami *et al.* for their Ni(OAc)₂/bipyridine system.^{22d} To test this hypothesis, we conducted a reaction under catalytic conditions but in the absence of aryl iodide (Scheme 5). 2,2'-Bibenzothiazole was obtained in 93% yield based on nickel (see ESI). A sacrificial amount of benzothiazole thus seems indeed necessary for the generation of the active species.

To get further insight into the mechanism, we also checked whether the biaryl coupling was the result of a true homogeneous process by conducting the coupling of benzothiazole with iodobenzene in the presence of 115 equiv. of Hg relatively to nickel (see ESI).²⁵ Formation of 2,2'-bibenzothiazole occurred in the same proportions as in a typical catalytic run. However, almost complete inhibition of the heterocoupling was observed (Scheme 6), thus suggesting that a process catalysed by nickel particles could follow the initial reduction of the nickel(II) pre-catalyst. Of note, the generation of such catalytically active nickel particles from **2c** could be compatible with the apparent long induction period observed with **2c** (51 % conv. after 16 h vs. 69 % after 18 h – Table 1, entries 2 and 6).

In addition, an experiment was performed in the presence of 5 mol% of the radical scavenger, TEMPO (see ESI). As seen in the run with Hg, formation of 2,2'-bibenzothiazole still occurred and that of 2-phenylbenzo[d]thiazole was almost completely suppressed (Scheme 6), thus suggesting that a radical pathway is also likely. All this draws a complicated picture with possible competing processes, among which a radical process catalysed by nickel particles might follow the

**Scheme 5** Dimerization of benzothiazole mediated by **2c****Scheme 6** Effect of additives

initial reduction of **2c** by the dimerization of a sacrificial amount of benzothiazole.

Conclusions

In summary, a series of four cationic *C,C*-(NHC-cyanoalkyl)-nickelacycles (**2a-d**) has been synthesized in high yield *via* optimized synthetic procedures involving: (i) the base-assisted activation of one of the C–H bond in α to the nitrile group of [NiXCP(NHC)] complexes that bear a cyanoalkyl chain bound to one of the nitrogen atom of the NHC ring⁵ and (ii) the subsequent removal of the Cp ligand from the resulting half-sandwich *C,C*-nickelacycles.³ Full characterization of **2a-d** coupled with a DFT structural analysis allowed us to establish that they bear *only one acetonitrile ligand per nickel atom* in the solid state, and suggests they exist as rare T-shaped 14-electron three-coordinate species.²

Application of these coordinatively and electronically unsaturated species bearing a robust anionic *C,C*-chelate in direct biaryl couplings between azoles and aryl halides, where nickel salts associated to classical neutral bidentate ligands have shown interesting results,²² proved relatively disappointing, the most active precatalyst, **2c**, showing only a modest activity for the coupling of a couple of azoles with a limited number of aryl iodides. Interestingly, control experiments suggest an initial reduction of the nickel(II) precatalyst by the dimerization of a sacrificial amount of benzothiazole that could either be followed by competing processes or by a radical process catalysed by nickel particles.

Experimental section

Materials and methods

All reactions were carried out using standard Schlenk or glovebox techniques under an atmosphere of dry argon. Solvents were distilled from appropriate drying agents under argon. Acetonitrile was freeze-pump-thaw degassed before use. Solution NMR spectra were recorded at 298 K on Bruker Ultra Shield 300, Bruker Spectrospin 400 or Bruker Avance III HD 500 spectrometers operating at 300.13, 400.14 or 500.14 MHz for ¹H and at 75.47, 100.61 or 125.77 MHz for ¹³C{¹H}. ¹H 2D COSY spectra were obtained for all complexes to help in the ¹H signal assignments. The assignments of ¹³C{¹H} NMR spectra were made with the aid of ¹H/¹³C heteronuclear single quantum coherence (HSQC) and/or ¹H/¹³C heteronuclear multiple-bond correlation (HMBC) for all complexes. The chemical shifts are referenced to the residual deuterated or ¹³C solvent peaks. Chemical shifts (δ) and coupling constants (*J*) are expressed in ppm and Hz respectively. IR spectra were recorded on a FT-IR Nicolet 380 or Perkin Elmer Spectrum Two spectrometer equipped with a diamond ATR. Vibrational frequencies are expressed in cm⁻¹. GC analyses were performed using *n*-dodecane as an internal standard with an Agilent 7820A instrument equipped with a HP-5 column. Elemental analyses were performed by the Service d'Analyses, de Mesures Physiques et de Spectroscopie Optique, UMR

CNRS 7177, Institut de Chimie, Université de Strasbourg. High resolution mass spectra were recorded on a Bruker micrOTOF-Q mass spectrometer by the Service de Spectrométrie de Masse, UMR CNRS 7177, Université de Strasbourg. Commercially available haloarenes and thiazoles as well as *n*-dodecane were distilled and stored under argon before use. [NiCp{Me-NHC-(CH₂)₂CN}] (**a**),⁵ [NiCp{Mes-NHC-(CH₂)₃CN}] (**c**),^{6a} and 5-phenyloxazole,²⁶ were prepared according to the published methods. The optimized syntheses of **1a** and **1c** are described hereafter; their spectroscopic data can be found in the previously published procedures.^{5,6a} The syntheses and characterizations of 1-(2,6-diisopropylphenyl)-3-butylnitrile-imidazolium chloride and 1-(2,4,6-trimethylphenyl)-3-propylnitrile-imidazolium bromide²⁷ are described in the supporting information.

Synthetic procedures

[NiBrCp{Mes-NHC-(CH₂)₂CN}] (b). Nickelocene (868 mg, 4.60 mmol) and 1-(2,4,6-trimethylphenyl)-3-propylnitrile-imidazolium bromide (981 mg, 3.06 mmol) were refluxed in THF (30 mL) for 4 days. The solution colour progressively turned from dark green to dark red. The reaction mixture was cooled to room temperature, and filtered through a Celite pad that was then rinsed with THF until the washings were colourless. The solvent was then removed under vacuum and the residue washed with pentane to remove the excess nickelocene. The resulting solid was then dried overnight under vacuum to afford **b** as a pink powder (802 mg, 1.81 mmol, 59 % yield). Anal. Calcd for C₂₀H₂₂N₃NiBr: C, 54.22; H, 5.01; N, 9.49. Found: C, 54.48; H, 4.97; N, 9.10. ¹H NMR (CDCl₃, 300.13 MHz): δ 7.37 (d, ³*J* = 1.5, 1H, NCH), 7.09 (s, 2H, *m*-H), 6.92 (d, ³*J* = 1.5, 1H, NCH), 5.30 (t, ³*J* = 6.0, 2H, NCH₂), 4.80 (s, 5H, C₅H₅), 3.44 (t, ³*J* = 6.0, 2H, CH₂CN), 2.43 (s, 3H, *p*-Me), 2.13 (s br., 6H, *o*-Me). ¹³C{¹H} NMR (CDCl₃, 75.47 MHz): δ 166.8 (NCN), 139.5, 136.6 and 136.0 (*o*-, *ipso*- and *p*-C_{Ar}), 129.4 (*m*-C_{Ar}), 124.6 (NCH), 123.2 (NCH), 117.7 (CN), 92.2 (C₅H₅), 48.0 (NCH₂), 21.3 (*p*-Me), 20.4 (CH₂CN), 18.7 (*o*-Me). IR [ATR]: ν (C_{sp2}-H) 3164 (w), 3131 (m), 3098 (w); ν (C_{sp3}-H) 2952 (w), 2910 (m), 2855 (w); ν (C≡N) 2253 (w).

[NiCp{DiPP-NHC-(CH₂)₃CN}] (d). Nickelocene (1.286 g, 6.81 mmol) and 1-(2,6-diisopropylphenyl)-3-butylnitrile-imidazolium chloride (1.508 g, 4.54 mmol) were refluxed in thf (45 mL) for 19 h. The solution colour progressively turned from dark green to purple-red. The reaction mixture was cooled to room temperature, diluted in THF (40 mL), and filtered through a Celite pad that was then rinsed with THF until the washings were colourless. The solvent was then removed under vacuum, and the residue washed with pentane to remove excess nickelocene. The pink powder was then dissolved in toluene, and filtered through a silica pad, that was rinsed with toluene until the washings were colourless. The resulting dark pink solution was then evaporated and the resulting solid dried overnight under vacuum, at 50 °C to afford **d** as a pink powder (1.124 g, 2.47 mmol, 54 %). Anal. Calcd for C₂₄H₃₀N₃NiCl: C, 63.40; H, 6.65; N, 9.24. Found: C, 63.43; H, 6.61; N, 9.24. ¹H NMR (CDCl₃, 300.13 MHz): δ 7.57 (t,

$^3J = 7.7$, 1H, *p*-H), 7.40 (d, $^3J = 7.7$, 2H, *m*-H), 7.21 (d, $^3J = 2.0$, 1H, NCH), 6.96 (d, $^3J = 2.0$, 1H, NCH), 5.20 (t, $^3J = 6.8$, 2H, NCH₂), 4.69 (s, 5H, C₅H₅), 2.60 (m, 6H, CH₂CH₂CN and CHMe₂), 1.37 (d, $^3J = 6.6$, 6H, CHMe₂), 1.05 (d, $^3J = 6.6$, 6H, CHMe₂). ¹³C{¹H} NMR (CDCl₃, 75.47 MHz): δ 165.7 (NCN), 146.8 (*o*-C_{Ar}), 136.4 (*ipso*-C_{Ar}), 130.5 (*p*-C_{Ar}), 125.8 (NCH), 124.3 (*m*-C_{Ar}), 122.1 (NCH), 119.1 (CN), 91.9 (C₅H₅), 50.7 (NCH₂), 28.4 (CHMe₂), 27.0 (CH₂), 26.4 (CHMe₂), 22.8 (CHMe₂), 15.1 (CH₂CN). IR [ATR]: ν(C_{sp2}-H) 3122 (w); ν(C_{sp3}-H) 2961 (m), 2926 (m), 2865 (m); ν(C≡N) 2245 (w).

[NiCp{Me-NHC-CH₂CH(CN)}] (1a).⁵ A 0.5 M solution of KHMDS in toluene (9.5 mL, 4.75 mmol) was added drop-wise to a dark red solution of **a** (1.842 g, 4.77 mmol) suspended in toluene (65 mL) at room temperature. The resulting dark olive mixture was stirred for 2 h and was filtered through an alumina column (5 x 3 cm) that was eluted with toluene and with THF to recover a dark green solution (note: the dark brown degradation products on the top of the alumina column rendered the filtration slow). The collected dark green solution was then evaporated under vacuum, and the residue washed with *n*-pentane (3 x 10 mL) and dried under vacuum overnight, to afford **1a** as a dark green powder (287 mg, 1.11 mmol, 23 %).

[NiCp{Mes-NHC-CH₂CH(CN)}] (1b). A 0.5 M solution of KHMDS in toluene (2.4 mL, 1.20 mmol) was added drop-wise to a dark pink solution of **b** (524 mg, 1.18 mmol) suspended in toluene (11 mL) at room temperature. The resulting dark olive mixture was stirred for 1 h and was filtered through a Celite pad that was rinsed with toluene until the washings were colourless (note: the dark brown degradation products on the top of the Celite pad rendered the filtration slow). The collected dark olive solution was then evaporated, and the residue was extracted with toluene and applied onto an alumina column (7 x 5 cm) that was eluted with toluene to give a light blue fraction, and with THF to recover a dark green solution. The dark green solution was then evaporated under vacuum, and the residue washed with *n*-pentane (3 x 3 mL) and dried under vacuum overnight, to afford **1b** as a green powder (121 mg, 0.334 mmol, 28 %). Anal. Calcd. for C₂₀H₂₁N₃Ni: C, 66.34; H, 5.85; N, 11.61. Found: C, 66.20; H, 5.89; N, 11.26. ¹H NMR (CDCl₃, 300.13 MHz): δ 6.99 (s, 1H, *m*-H), 6.97 (s, 1H, *m*-H), 6.96 (d, $^3J = 2.0$, 1H, NCH), 6.62 (d, $^3J = 2.0$, 1H, NCH), 4.77 (s, 5H, C₅H₅), 3.89 (m, 2H, NCH₂), 2.75 (dd, $^3J = 7.8$, $^3J = 6.0$, 1H, CHCN), 2.35 (s, 3H, *p*-Me), 2.08 (s, 3H, *o*-Me), 2.01 (s, 3H, *o*-Me). ¹³C{¹H} NMR (CDCl₃, 75.47 MHz): δ 175.9 (NCN), 139.4, 136.4, 136.1 and 135.5 (*p*-, *ipso*-, *o*-C_{Ar}), 131.5 (CN), 129.1 (*m*-C_{Ar}), 128.9 (*m*-C_{Ar}), 122.1 (NCH), 117.7 (NCH), 90.0 (C₅H₅), 54.2 (NCH₂), 21.3 (*p*-Me), 18.0 (*o*-Me), 17.8 (*o*-Me), -11.0 (CHCN). IR [ATR]: ν(C_{sp2}-H) 3153 (w), 3127 (m); ν(C_{sp3}-H) 2952 (w), 2919 (m), 2856 (w); ν(C≡N) 2185 (s).

[NiCp{Mes-NHC-(CH₂)₂CH(CN)}] (1c).^{6a} A 0.5 M solution of KHMDS in toluene (5.78 mL, 2.89 mmol) was added drop-wise to a dark pink solution of **c** (1.193 mg, 2.89 mmol) suspended in toluene (24 mL) at room temperature. The resulting dark olive mixture was stirred for 2 h and was filtered through a Celite pad that was rinsed with toluene until the washings were colourless (note: the dark brown degradation products

on the top of the Celite pad rendered the filtration slow). The collected dark green solution was then evaporated under vacuum, and the residue washed with *n*-pentane (3 x 10 mL) and dried under vacuum overnight, to afford **1c** as a dark green powder (715 mg, 1.90 mmol, 66 %).

[NiCp{DiPP-NHC-(CH₂)₂CH(CN)}] (1d). A 0.5 M solution of KHMDS in toluene (5 mL, 2.50 mmol) was added drop-wise to a dark pink solution of **d** (1.124 g, 2.47 mmol) in toluene (20 mL) at room temperature. The resulting dark green mixture was stirred for 1 h and was filtered through a Celite pad that was rinsed with toluene until the washings were colourless (note: the dark brown degradation products on the top of the Celite pad rendered the filtration slow). The collected dark green solution was then evaporated under vacuum, and the residue washed with pentane (3 x 10 mL) and dried under vacuum for 3 h to afford **1d** as a green powder (665 mg, 1.59 mmol, 64 %). Anal. Calcd. for C₂₄H₂₉N₃Ni: C, 68.93; H, 6.99; N, 10.05. Found: C, 69.19; H, 7.01; N, 10.02. ¹H NMR (CDCl₃, 300.13 MHz): δ 7.49 (t, $^3J = 7.8$, 1H, *p*-H), 7.34 (dd, $^3J = 7.8$, $^4J = 1.4$, 1H, *m*-H), 7.27 (dd, $^3J = 7.8$, $^4J = 1.4$, 1H, *m*-H), 7.05 (d, $^3J = 2.1$, 1H, NCH), 6.73 (d, $^3J = 2.1$, 1H, NCH), 4.67 (s, 5H, C₅H₅), 4.01 (m, 1H, NCH₂), 3.84 (m, 1H, NCH₂), 2.78 (sept, $^3J = 6.9$, 1H, CHMe₂), 2.44 (sept, $^3J = 6.9$, 1H, CHMe₂), 2.15 (t, $^3J = 6.6$, 1H, CHCN), 1.68 (m, 1H, CH₂), 1.51 (d, $^3J = 6.9$, 3H, CHMe₂), 1.43 (m, 1H, CH₂), 1.34 (d, $^3J = 6.9$, 3H, CHMe₂), 1.07 (d, $^3J = 6.9$, 3H, CHMe₂), 1.02 (d, $^3J = 6.9$, 3H, CHMe₂). ¹³C{¹H} NMR (CDCl₃, 75.47 MHz): δ 172.6 (NCN), 146.9 and 145.8 (*o*-C_{Ar}), 137.2 (*ipso*-C_{Ar}), 132.5 (CN), 130.1 (*p*-C_{Ar}), 124.2 (NCH), 123.8 and 123.7 (*m*-C_{Ar}), 121.6 (NCH), 91.2 (C₅H₅), 50.3 (NCH₂), 30.2 (CH₂), 28.7 and 28.3 (CHMe₂), 25.9 and 25.7 (CHMe₂), 22.7 and 22.7 (CHMe₂), -25.1 (CHCN). IR [ATR]: ν(C_{sp2}-H) 3140 (w); ν(C_{sp3}-H) 2951 (m), 2924 (w), 2862 (w); ν(C≡N) 2179 (m).

[Ni{Me-NHC-CH₂CH(CN)}(NCCH₃)]⁺PF₆⁻ (2a). Aqueous HCl (37%) diluted in acetonitrile to 1.0 M (1.06 mL, 1.06 mmol) was added drop-wise to an equimolar amount of a dark green suspension of **1a** (277 mg, 1.07 mmol) and KPF₆ (196 mg, 1.06 mmol) in acetonitrile (16 mL) at 0 °C. The reaction mixture rapidly turned ochre yellow and was stirred for 10 min at 0 °C before being warmed to room temperature and filtered on a Celite pad, which was subsequently rinsed with acetonitrile until the washings were colourless. Volatiles were evaporated under vacuum, and the resulting solid was washed with pentane (3 x 3 mL), and dried overnight under vacuum at room temperature to afford **2a** as a dark yellow solid (380 mg, 1.00 mmol, 95%). Anal. Calcd for C₉H₁₁F₆N₄NiP: C, 28.53; H, 2.93; N, 14.79. Found: C, 28.78; H, 3.00; N, 12.99. Repeated attempts to obtain correct elemental analyses gave low nitrogen values. HR-MS (ESI): *m/z* [M]⁺ calcd for C₉H₁₁N₄Ni 233.0332, found 233.0328. ¹H NMR (CD₃CN, 400.14 MHz): δ 7.07 (d, $^3J = 2.0$, 1H, NCH), 6.90 (d, $^3J = 2.0$, 1H, NCH), 3.86 (dd, $^2J = 12.8$, $^3J = 7.6$, 1H, NCH₂), 3.62 (s, 3H, NMe), 3.55 (dd, $^2J = 12.8$, $^3J = 2.8$, 1H, NCH₂), 2.59 (m, 1H, CHCN), 1.96 (s, 3H, free CH₃CN). ¹H NMR (C₅D₅N, 300.13 MHz): δ 7.19 (s, 1H, NCH), 6.94 (s, 1H, NCH), 3.81 (m, 2H, NCH₂), 2.49 (s, 3H, NMe), 2.42 (br., 1H, CHCN), 1.83 (s, 3H, CH₃CN). ¹³C{¹H} NMR (CD₃CN, 100.61 MHz): δ 156.6 (br., NCN), 126.2 and 119.1 (NCH), 52.4 (NCH₂), 37.7 (NMe), 7.1 (br., CHCN). ¹³C{¹H} NMR (C₅D₅N,

125.77 MHz): δ 161.0 (NCN), 128.8 and 128.4 (CH₃CN and CHCN) 126.3 and 119.1 (NCH), 52.8 (NCH₂), 35.4 (NMe), 8.9 (br. CHCN), 1.8 (CH₃CN). IR [ATR]: ν (C_{sp2}-H) 3174 (w), 3149 (w); ν (C_{sp3}-H) 2951 (w); ν (C≡N) 2239 (m); ν (P-F) 823 (s).

[Ni{Mes-NHC-CH₂CH(CN)}(NCCH₃)⁺PF₆⁻ (2b). Aqueous HCl (37%) diluted in acetonitrile to 1.0 M (0.13 mL, 0.130 mmol) was added drop-wise to an equimolar amount of a dark green suspension of **1b** (48 mg, 0.133 mmol) and KPF₆ (23 mg, 0.125 mmol) in acetonitrile (2 mL) at 0 °C. The reaction mixture rapidly turned ochre yellow and was stirred for 10 min at 0 °C, before being warmed to room temperature and filtered on a Celite pad that was rinsed with acetonitrile until the washings were colourless. Volatiles were evaporated under vacuum, and the resulting solid was washed with pentane (3 x 2 mL), and dried overnight under vacuum at room temperature to afford **2b** as a dark yellow solid (52 mg, 0.108 mmol, 86 %). Anal. Calcd for C₁₇H₁₉F₆N₄NiP: C, 42.27; H, 3.97; N, 11.60. Found: C, 41.68; H, 4.07; N, 11.30. HR-MS (ESI): m/z [M]⁺ calcd for C₁₇H₁₉N₄Ni 337.0958, found 337.0985. ¹H NMR (CD₃CN, 500.15 MHz): δ 7.32 (s, 1H, NCH), 7.07 (s, 1H, *m*-H), 7.02 (s, 1H, *m*-H), 6.89 (d, 1H, NCH), 3.96 (dd, ²*J* = 12.5, ³*J* = 7.5, 1H, NCH₂), 3.67 (m, 1H, NCH₂), 2.65 (m, 1H, CHCN), 2.29 (s, 3H, *p*-Me), 2.20 (br. s, 3H, *o*-Me), 2.06 (s, 3H, *o*-Me), 1.97 (s, 3H, free CH₃CN). ¹H NMR (C₅D₅N, 300.13 MHz): δ 7.58 (d, ³*J* = n.r., 1H, NCH), 7.01 (d, ³*J* = 1.8, 1H, NCH), 6.59 (s, 1H, *m*-H), 6.31 (s, 1H, *m*-H), 4.15 (dd, ²*J* = 12.6, ³*J* = 7.5, 1H, NCH₂), 3.92 (dd, ²*J* = 12.6, ³*J* = 3.0, 1H, NCH₂), 2.29 (dd, ³*J* = 7.5, ³*J* = 3.0, 1H, CHCN), 2.21 (s, 3H, *o*-Me), 2.06 (s, 3H, *p*-Me), 1.86 (s, 6H, *o*-Me and free CH₃CN). ¹³C{¹H} NMR (CD₃CN, 125.77 MHz): δ 158.6 (br., NCN), 140.6, 136.5, 136.2, 135.8 (*ipso*-, *p*-, *o*-C_{Ar}), 130.0 and 129.8 (*m*-C_{Ar}), 125.5 and 120.4 (NCH), 53.1 (NCH₂), 21.0 (*p*-Me), 17.9 and 17.6 (*o*-Me), 7.8 (CHCN). ¹³C{¹H} NMR (C₅D₅N, 125.77 MHz): δ 162.8 (NCN), 139.7, 135.2, 134.7, 134.3 (*ipso*-, *p*-, *o*-C_{Ar}), 129.8 (*m*-C_{Ar}), 126.6 (CHCN), 125.7 and 120.4 (NCH), 117.9 (free CH₃CN), 53.2 (NCH₂), 20.9 (*p*-Me), 18.1 and 17.9 (*o*-Me), 9.7 (CHCN), 1.4 (free CH₃CN). IR [ATR]: ν (C_{sp2}-H) 3169 (w), 3144 (w); ν (C_{sp3}-H) 2941 (w), 2924 (w), 2864 (w); ν (C≡N) 2243 (m); ν (P-F) 829 (s).

[Ni{Mes-NHC-(CH₂)₂CH(CN)}(NCCH₃)⁺PF₆⁻ (2c). Aqueous HCl (37%) diluted in acetonitrile to 1.0 M (1.30 mL, 1.30 mmol) was added drop-wise to an equimolar amount of a dark green suspension of **1c** (536 mg, 1.30 mmol) and KPF₆ (239 mg, 1.30 mmol) in acetonitrile (10 mL) at 0 °C. The reaction mixture rapidly turned ochre yellow and was stirred for 10 min at 0 °C, before being warmed to room temperature and filtered on a Celite pad that was rinsed with acetonitrile until the washings were colourless. Volatiles were evaporated under vacuum, and the resulting solid was washed with pentane (3 x 10 mL) and dried overnight under vacuum at 50 °C to afford **2c** as a dark yellow solid (627 mg, 1.26 mmol, 97%). Anal. Calcd for C₁₈H₂₁F₆N₄NiP: C, 43.50; H, 4.26; N, 11.27. Found: C, 43.49; H, 4.31; N, 10.82. HR-MS (ESI): m/z [M]⁺ calcd for C₁₈H₂₁N₄Ni 351.1114, found 351.1126. ¹H NMR (CD₃CN, ca. 0.1 M, ²⁸500.14 MHz): δ 7.32 (s, 1H, NCH), 7.30 (br., 1H, *m*-H), 7.07 (s, 1H, *m*-H), 7.04 (s, 1H, NCH), 4.13 and 4.03 (2m, 2 x 1H, NCH₂), 2.57 (s, 3H, *o*-Me), 2.42 (br. s, 4H, *p*-Me and CHCN), 2.03 (s, 3H, *o*-Me), 1.96 (s, 3H, free CH₃CN), 1.67 (br., 1H, NCH₂CH₂), 1.05 (br., 1H, NCH₂CH₂). ¹H NMR (C₅D₅N, 300.13 MHz): δ 7.58

(d, ³*J* = n.r., 1H, NCH), 7.1 (d, ³*J* = 1.8, 1H, NCH), 6.89 (s, 1H, *m*-H), 6.41 (s, 1H, *m*-H), 4.41 (m, 1H, NCH₂), 4.30 (m, 1H, NCH₂), 2.81 (s, 3H, *o*-Me), 2.20 (s, 3H, *p*-Me), 2.01 (dd, 1H, ³*J* = 8.1, ³*J* = 6.9, CHCN), 1.86 (s, 3H, free CH₃CN), 1.82 (m, 1H, CH₂), 1.46 (s, 3H, *o*-Me), 1.29 (m, 1H, CH₂). ¹³C{¹H} NMR (CD₃CN, 125.77 MHz): δ 155.4 (br., NCN); 140.4, 136.5, 136.2, 135.7 (*ipso*-, *p*-, *o*-C_{Ar}), 130.4 and 130.1 (*m*-C_{Ar}), 125.5 and 123.7 (NCH), 50.5 (NCH₂), 29.2 (CH₂), 21.1 (*p*-Me), 19.1 and 18.3 (*o*-Me), -2.0 (br., CHCN). ¹³C{¹H} NMR (C₅D₅N, 125.77 MHz): δ 161.9 (NCN), 139.6, 134.4, (*ipso*-, *p*- or *o*-C_{Ar}), 130.5 and 130.0 (*m*-C_{Ar}), 128.1 (CHCN), 125.0 (NCH), 118.0 (free CH₃CN), 50.9 (NCH₂), 30.3 (CH₂), 21.1 (*p*-Me), 19.8 and 18.4 (*o*-Me), 1.5 (free CH₃CN), 0.9 (CHCN). IR [ATR]: ν (C_{sp2}-H) 3174 (w), 3146 (w); ν (C_{sp3}-H) 2943 (w), 2922 (w), 2862 (w); ν (C≡N) 2236 (m); ν (P-F) 829 (s).

[Ni{DiPP-NHC-(CH₂)₂CH(CN)}(NCCH₃)⁺PF₆⁻ (2d). Aqueous HCl (37%) diluted in acetonitrile to 1.0 M (0.43 mL, 0.430 mmol) was added drop-wise to an equimolar amount of a dark green suspension of **1d** (207 mg, 0.495 mmol) and KPF₆ (79 mg, 0.429 mmol) in acetonitrile (4 mL) at 0 °C. The reaction mixture rapidly turned ochre yellow and was stirred for 10 min at 0 °C, before being warmed to room temperature and filtered on a Celite pad that was rinsed with acetonitrile until the washings were colourless. Volatiles were evaporated under vacuum, and the resulting solid was washed with pentane (3 x 3 mL), and dried overnight under vacuum at room temperature to afford **2d** as a dark yellow solid (200 mg, 0.371 mmol, 86 %). Anal. Calcd for C₂₁H₂₇F₆N₄NiP: C, 46.78; H, 5.05; N, 10.39. Found: C, 46.72; H, 5.33; N, 10.19. HR-MS (ESI): m/z [M]⁺ calcd for C₂₁H₂₇N₄Ni 393.1584, found 393.1604. ¹H NMR (CD₃CN, 400.14 MHz): δ 7.50 (d, ³*J* = 5.4, 1H, *m*-H), 7.50 (d, ³*J* = 4.0, 1H, *m*-H), 7.35 (dd, ³*J* = 5.4, ³*J* = 4.0, 1H, *p*-H), 7.32 (d, ³*J* = 1.4, 1H, NCH), 7.11 (d, ³*J* = 1.4, 1H, NCH), 4.09 (m, 2H, NCH₂), 3.42 (sept, 1H, CHMe₂), 2.50 (sept, ³*J* = 6.8, 1H, CHMe₂), 2.28 (t, ³*J* = 6.4, 1H, CHCN), 1.96 (s, 3H, free CH₃CN), 1.89 (d, ³*J* = 6.8, 3H, CHMe₂), 1.75 (m, 1H, CH₂), 1.24 (d, ³*J* = 6.8, 3H, CHMe₂), 1.16 (d, ³*J* = 6.8, 3H, CHMe₂), 1.15 (m, 1H, CH₂), 1.13 (d, ³*J* = 6.8, 3H, CHMe₂). ¹H NMR (C₅D₅N, 300.13 MHz): δ 7.62 (d, ³*J* = 1.4, 1H, NCH), 7.53 (m, 2H, *m*-H), 7.45 (d, ³*J* = 1.4, 1H, NCH), 6.97 (dd, ³*J* = 6.6, ³*J* n.r., 1H, *p*-H), 4.54 (m, 2H, NCH₂ and CHMe₂), 4.40 (m, 1H, NCH₂), 2.08 (d, ³*J* = 6.6, 3H, CHMe₂), 2.00 (m, 2H, CHMe₂ and CHCN), 1.85 (s, 3H, free CH₃CN), 1.30 (m, 2H, CH₂), 1.04 (d, ³*J* = 6.6, 3H, CHMe₂), 0.98 (d, ³*J* = 6.6, 3H, CHMe₂), 0.38 (d, ³*J* = 6.8, 3H, CHMe₂). ¹³C{¹H} NMR (CD₃CN, 100.61 MHz): δ 153.8 (br., NCN), 146.9 and 146.2 (*o*-C_{Ar}), 136.4 (*ipso*-C_{Ar}), 131.4 (*m*-C_{Ar}), 126.9 (NCH), 125.4 and 125.2 (*p*- and *m*-C_{Ar}), 123.6 (NCH), 49.8 (NCH₂), 29.7 and 29.1 (CHMe₂), 28.1 (CH₂), 25.3, 25.1, 24.4 and 23.5 (CHMe₂), -2.7 (br. CHCN). ¹³C{¹H} NMR (C₅D₅N, 125.77 MHz): δ 161.8 (NCN), 146.3 and 145.9 (*o*-C_{Ar}), 131.0 (*m*-C_{Ar}), 127.9 (CHCN), 127.2 (NCH), 125.2 (*p*- or *m*-C_{Ar}), 123.1 (NCH), 118.0 (free CH₃CN), 50.9 (NCH₂), 30.3 (CHMe₂), 28.4 (CH₂), 26.7, 25.6, 24.0 and 22.6 (CHMe₂), 1.4 (free CH₃CN), 0.8 (CHCN). IR [ATR]: ν (C_{sp2}-H) 3179 (w), 31464 (w); ν (C_{sp3}-H) 2966 (m), 2922 (m), 2867 (m); ν (C≡N) 2233 (m); ν (P-F) 834 (s).

Typical procedure for the heteroarylation of aryl halides. An oven dried Schlenk tube equipped with a magnetic stir bar was charged with **2c** (10 mg, 0.0201 mmol), LiOt-Bu (59 mg, 0.737 mmol, 2.0 equiv.), benzothiazole (40 μ L, 0.369 mmol, 1.0

equiv.), iodobenzene (60 μL , 0.536 mmol, 1.5 equiv.), dodecane (15 μL , 0.066 mmol), and 1,4-dioxane (3 mL), and sealed. The Schlenk tube was then introduced into an oil bath that was heated up to a temperature of 140 $^{\circ}\text{C}$. After 36 h, the reaction medium was cooled to room temperature, and the volatiles were evaporated under high vacuum. The resulting brown residue was extracted with diethyl ether and filtered over a silica pad (2.5 \times 1 cm). The collected filtrate was then concentrated under vacuum, and loaded onto a silica column (Merck Silica Gel 60 - mesh size 40-60 μm ; 28 \times 3.5 cm) pre-wet with petroleum ether (bp. 40-70 $^{\circ}\text{C}$). Elution with a petroleum ether/ethyl acetate mixture (benzothiazole derivatives: 98/2; other azoles: 90/10) afforded the coupling product.

X-ray diffraction studies

Single crystals of **1a** and **1b** suitable for X-ray diffraction studies were obtained from slow evaporation of a concentrated solution in THF at room temperature. Diffraction data were collected at 173(2) K on a Bruker APEX II DUO Kappa CCD area detector diffractometer equipped with an Oxford Cryosystem liquid N_2 device using Mo- $\text{K}\alpha$ radiation ($\lambda = 0.71073 \text{ \AA}$). A summary of crystal data, data collection parameters and structure refinements is given in Table S1. The crystal-detector distance was 38 mm. The cell parameters were determined (APEX2 software) from reflections taken from three sets of twelve frames, each at ten seconds exposure. The structure was solved using direct methods with SHELXS-97 and refined against F^2 for all reflections using the SHELXL-97 software.²⁹ A semi-empirical absorption correction was applied using SADABS in APEX II.³⁰ All non-hydrogen atoms were refined with anisotropic displacement parameters, using weighted full-matrix least-squares on F^2 . Hydrogen atoms were included in calculated positions and treated as riding atoms using SHELXL default parameters.

DFT computational details

Calculations were performed using the Gaussian 09 software package³¹ and the PBE0 functional, without symmetry constraints. That functional uses a hybrid generalized gradient approximation (GGA), including 25 % mixture of Hartree-Fock³² exchange with DFT³³ exchange-correlation, given by Perdew, Burke and Ernzerhof functional (PBE).³⁴ The basis set used for geometry optimizations (b1) consisted of the Stuttgart/Dresden ECP (SDD) basis set³⁵ augmented with a f-polarization function³⁶ to describe the electrons of Ni, and a standard 6-31G(d,p) basis set³⁷ for all other atoms. The transition state optimization was performed with the Synchronous Transit-Guided Quasi-Newton Method (STQN) developed by Schlegel *et al.*,³⁸ following extensive searches of the Potential Energy Surface. Frequency calculations were performed to confirm the nature of the stationary points, yielding one imaginary frequency for the transition state and none for the minima. The transition state was further confirmed by following its vibrational mode downhill on both sides and obtaining the minima presented on the energy

profile. The electronic energies (Eb1) obtained at the PBE0/b1 level of theory were converted to free energy at 298.15 K and 1 atm (Gb1) by using zero point energy and thermal energy corrections based on structural and vibration frequency data calculated at the same level.

Single point energy calculations were performed on the geometries obtained at the PBE0/b1 level using the M06 functional, and a 6-311++G(d,p) basis set.^{37,39} The M06 functional is a hybrid meta-GGA functional developed by Truhlar and Zhao,⁴⁰ and it was shown to perform very well for the kinetics of transition metal molecules, providing a good description of weak and long range interactions.⁴¹ Solvent effects (MeCN) were accounted for in the M06/6-311++G(d,p)//PBE0/b1 calculations by means of the Polarizable Continuum Model (PCM) initially devised by Tomasi and coworkers⁴² with radii and non-electrostatic terms of the SMD solvation model, developed by Truhlar and co-workers.⁴³

The free energy values presented (Gb2soln) were derived from the electronic energy values obtained at the M06/6-311++G(d,p)//PBE0/b1 level, including solvent effects (Eb2soln), according to the following expression: Gb2soln = Eb2soln + Gb1 - Eb1.

The calculated frequencies for the CN stretch in all species were corrected with a scale factor of 0.932 resulting from the comparison of the calculated and experimental CN frequency values observed for **1a**. Presented calculated frequency spectra were drawn with the Chemcraft program⁴⁴ and a Lorentzian line broadening of 30 % at peak half-width to account for thermal line broadening.

Conflict of interest

There are no conflicts to declare.

Acknowledgements

We are grateful to the Université de Strasbourg and the CNRS for their financial help. VR thanks the Agence Nationale de la Recherche (ANR 2010 JCJC 716 1; SBA-15-NHC-NiCat) for the post-doctoral fellowship of S. Shahane. The "Investissements d'avenir" program of the Université de Strasbourg is acknowledged for the doctoral fellowship of B. de P. Cardoso. We appreciate the assistance of Corinne Bailly for the structural determinations of **1a** and **1b**, and of Dr. Philippe Bertani for the ^{13}C CP-MAS NMR spectrum of **2c**. LfV acknowledges the Fundação para a Ciência e Tecnologia, FCT UID/QUI/00100/2013, for funding.

Notes and references

‡ Isolated yields of **2a-d** have been calculated for molecules containing one acetonitrile ligand.

§ We mentioned in our preliminary communication that the ^1H NMR spectrum of **2c** is concentration dependent. This is also observed for **2a,b,d**, though to a much lesser extent. A VT NMR experiment run from +27 $^{\circ}\text{C}$ to +75 $^{\circ}\text{C}$ on a diluted solution of **2c** in CD_3CN did not result in significant changes.

§§ The solid-state ^{13}C CP-MAS NMR spectrum of **2c** displays broad signals in the expected diamagnetic area, *i.e.*: at similar chemical shifts than those of the solution ^{13}C NMR peaks.

§§§ The triplet state is $16.0\text{ kcal.mol}^{-1}$ less stable than the singlet state for **2a**, and $19.9\text{ kcal.mol}^{-1}$ less stable for **2c**.

§§§§ A stabilizing interaction between the PF_6^- counteranion and the cationic nickel centre cannot be excluded. However the solid state FTIR spectra of **2a-d** all show a P–F stretch in the same frequency range (*ca.* 830 cm^{-1}) and with the same shape as observed in $[\text{Ni}(\eta^5\text{-C}_5\text{R}_5)(\text{NHC})(\text{NCMe})]^+\text{PF}_6^-$ complexes where no such interaction is found.^{6a}

- M. A. Ortuño, S. Conejero and A. Lledós, *Beilstein J. Org. Chem.*, 2013, **9**, 1352.
- (a) C. A. Laskowski and G. L. Hillhouse, *J. Am. Chem. Soc.*, 2008, **130**, 13846; (b) T. Tamaki, M. Nagata, M. Ohashi and S. Ogoshi, *Chem. Eur. J.*, 2009, **15**, 10083; (c) C. A. Laskowski, G. R. Morello, C. T. Saouma, T. R. Cundari and G. L. Hillhouse, *Chem. Sci.*, 2013, **4**, 170; (d) Y. Hoshimoto, T. Ohata, M. Ohashi and S. Ogoshi, *Chem. Eur. J.*, 2014, **20**, 4105; (e) S. Pelties and R. Wolf, *Organometallics*, 2016, **35**, 2722.
- M. Henrion, A. M. Oertel, V. Ritleng and M. J. Chetcuti, *Chem. Commun.*, 2013, **49**, 6424.
- (a) C. D. Abernethy, A. H. Cowley and R. A. Jones, *J. Organomet. Chem.*, 2000, **596**, 3; (b) V. Ritleng, E. Brenner and M. J. Chetcuti, *J. Chem. Educ.*, 2008, **85**, 1646; (c) S. Milosevic, E. Brenner, V. Ritleng and M. J. Chetcuti, *Dalton Trans.*, 2008, 1973; (d) J. Cooke, O. C. Lightbody, *J. Chem. Educ.*, 2011, **88**, 88; (e) A. M. Oertel, V. Ritleng and M. J. Chetcuti, *Organometallics*, 2012, **31**, 2829.
- A. M. Oertel, J. Freudenreich, J. Gein, V. Ritleng, L. F. Veiros and M. J. Chetcuti, *Organometallics*, 2011, **30**, 3400.
- (a) A. M. Oertel, V. Ritleng, M. J. Chetcuti and L. F. Veiros, *J. Am. Chem. Soc.*, 2010, **132**, 13588; (b) A. M. Oertel, V. Ritleng, A. Busiah, L. F. Veiros and M. J. Chetcuti, *Organometallics*, 2011, **30**, 6495.
- (a) W. A. Herrmann, O. Runte and G. Artus, *J. Organomet. Chem.*, 1995, **501**, C1. (b) M. V. Baker, P. J. Barnard, S. K. Brayshaw, J. L. Hickey, B. W. Skelton and A. H. White, *Dalton Trans.*, 2005, 37. (c) E. S. Chernyshova, R. Goddard and K.-R. Pörschke, *Organometallics*, 2007, **26**, 3236. (d) Q. Teng and H. V. Huynh, *Dalton Trans.*, 2017, **46**, 614.
- C. Jandl and A. Pöthig, *Chem. Commun.*, 2017, **53**, 2098.
- (a) S. J. Anderson, F. J. Wells, G. Wilkinson, B. Hussain and M. B. Hursthouse, *Polyhedron*, 1988, **7**, 2615; (b) J. Barrera, M. Sabat and W. D. Harman, *J. Am. Chem. Soc.*, 1991, **113**, 8178; (c) J. Barrera, M. Sabat and W. D. Harman, *Organometallics*, 1993, **12**, 4381; (d) S. Thomas, E. R. T. Tiekink and C. G. Young, *Organometallics*, 1996, **15**, 2428; (e) S. Thomas, C. G. Young and E. R. T. Tiekink, *Organometallics*, 1998, **17**, 182; (f) H. Wadepohl, U. Arnold, H. Pritzkow, M. J. Calhorda and L. F. Veiros, *J. Organomet. Chem.*, 1999, **587**, 233.
- C. Jandl, S. Stegbauer and A. Pöthig, *Acta Cryst C*, 2016, **72**, 509.
- For $\mu_2\text{-}\eta^2, \eta^2$ -crosswire bridging acetonitrile ligands with group 6 metals, see: (a) J. L. Eglin, E. M. Hines, E. J. Valente and J. D. Zubkowski, *Inorg. Chim. Acta*, 1995, **229**, 113; (b) F. A. Cotton and F. E. Kühn, *J. Am. Chem. Soc.*, 1996, **118**, 5826; (c) F. A. Cotton, L. M. Daniels, C. A. Murillo and X. Wang, *Polyhedron*, 1998, **17**, 2781.
- For $\mu_2\text{-}\eta^1, \eta^1$ -bridging acetonitrile ligands with alkali metals, lanthanides, and group 4, 11 and 12 metals, see: (a) W. J. Evans, M. A. Greci and J. W. Ziller, *Chem. Commun.*, 1998, 2367; (b) J. D. Beckwith, M. Tschinkl, A. Picot, M. Tsunoda, R. Bachman and F. P. Gabbaï, *Organometallics*, 2001, **20**, 3169; (c) P. Lin, W. Clegg, R. W. Harrington and R. A. Henderson, *Dalton Trans.*, 2005, 2349; (d) M. R. A. Al-Mandhary, C. M. Fitchett and P. J. Steel, *Aust. J. Chem.*, 2006, **59**, 307; (e) C. Lorber, R. Choukroun and L. Vendier, *Organometallics*, 2008, **27**, 5017; (f) T. C. Davenport and T. D. Tilley, *Angew. Chem. Int. Ed.*, 2011, **50**, 12205.
- For a $\mu_3\text{-}\eta^1, \eta^1, \eta^1$ -bridging acetonitrile ligand with Hg, see: I. A. Tikhonova, F. M. Dolgushin, A. I. Yanovsky, Z. A. Starikova, P. V. Petrovskii, G. G. Furin and V. B. Shur, *J. Organomet. Chem.*, 2000, **613**, 60.
- For a $\mu_3\text{-}\eta^2, \eta^2$ -bridging acetonitrile ligand with Nb, see: H. A. N. Joensen, G. K. Hansson, S. G. Kozlova, A. L. Gushchin, I. Sjøtofte and B.-L. Ooi, *Inorg. Chem.*, 2010, **49**, 1720.
- D. Walther, H. Schönberg, E. Dinjus and J. Sieler, *J. Organomet. Chem.*, 1987, **334**, 377.
- For another example of μ_2, η^1, η^2 -acetonitrile ligand with Mn, see: F. J. García Alonso, M. García Sanz, V. Riera, A. Anillo Abril, A. Tripicchio and F. Ugozzoli, *Organometallics*, 1992, **11**, 801.
- In a formally saturated complex, the side-on nitrile is viewed as a classic two-electron donor: T. C. Wright, G. Wilkinson, M. Motevalli and M. B. Hursthouse, *J. Chem. Soc., Dalton Trans.*, 1986, 2017.
- G. Rouschias and G. Wilkinson, *J. Chem. Soc. A*, 1968, 489.
- H. Endres, In: *Comprehensive Coordination Chemistry*, Vol. 2, Eds.: G. Wilkinson, R. D. Gillard and J. A. McCleverty, Pergamon, Oxford, 1987, p. 261.
- Three-coordinate Y-shaped Ni(II) complexes are generally paramagnetic, see for instance: (a) P. L. Holland, T. R. Cundari, L. L. Perez, N. A. Eckert and R. J. Lachiotte, *J. Am. Chem. Soc.*, 2002, **124**, 14416; (b) N. J. Hartmann, G. Wu and T. W. Hayton, *Angew. Chem. Int. Ed.*, 2015, **54**, 14956.
- (a) J. Yamaguchi, K. Muto, K. Itami, *Eur. J. Org. Chem.*, 2013, 19. (b) S. A. Johnson, *Dalton Trans.*, 2015, **44**, 10905. (c) N. Chatani, *Nickel-Catalyzed C–H Bond Functionalization Utilizing an N,N'-Bidentate Directing Group*. In: *C–H Bond Activation and Catalytic Functionalization II. Topics in Organometallic Chemistry*. Vol. 56, P. Dixneuf and H. Doucet (eds), Springer, 2015.
- (a) J. Canivet, J. Yamaguchi, I. Ban and K. Itami, *Org. Lett.*, 2009, **11**, 1733; (b) H. Hachiya, K. Hirani, T. Satoh and M. Miura, *Org. Lett.*, 2009, **11**, 1737; (c) O. Kobayashi, D. Uruguchi and T. Yamakawa, *Org. Lett.*, 2009, **11**, 2679; (d) T. Yamamoto, K. Muto, M. Komiyama, J. Canivet, J. Yamaguchi and K. Itami, *Chem. Eur. J.*, 2011, **17**, 10113.
- (a) K. Muto, J. Yamaguchi and K. Itami, *J. Am. Chem. Soc.*, 2012, **134**, 169; (b) K. Muto, J. Yamaguchi, A. Lei and K. Itami, *J. Am. Chem. Soc.*, 2013, **135**, 16384; (c) J. Wang, D. M. Ferguson and D. Kalyani, *Tetrahedron*, 2013, **69**, 5780; (d) H. Xu, K. Muto, J. Yamaguchi, C. Zhao, K. Itami and D. G. Musaev, *J. Am. Chem. Soc.*, 2014, **136**, 14834; (e) K. Muto, T. Hatakeyama, J. Yamaguchi and K. Itami, *Chem. Sci.*, 2015, **6**, 6792; (f) Y. Wang, S.-B. Wu, W.-J. Shi and Z.-J. Shi, *Org. Lett.*, 2016, **18**, 2548.
- (a) K. Amaike, K. Muto, J. Yamaguchi and K. Itami, *J. Am. Chem. Soc.*, 2012, **134**, 13573; (b) A. Kruckenberg, H. Wadepohl and L. H. Gade, *Organometallics*, 2013, **32**, 5153; (c) L. Meng, Y. Kamada, K. Muto, J. Yamaguchi and K. Itami, *Angew. Chem. Int. Ed.*, 2013, **52**, 10048.
- J. A. Widegren and R. G. Finke, *J. Mol. Cat. A*, 2003, **198**, 317.
- F. Besselièvre, F. Mahuteau-Betzer, D. S. Grierson and S. Piguel, *J. Org. Chem.*, 2008, **73**, 3278.
- H. V. Huynh and J. Wu, *J. Organomet. Chem.*, 2009, **694**, 323.
- For a ^1H NMR spectrum at $3.10^{-2}\text{ mol.L}^{-1}$ see ref. 3.
- (a) G. M. Sheldrick, SHELXL-97, *Program for Crystal Structure Analysis (Release 97-2)*, 1998. Göttingen, Germany; (b) G. M. Sheldrick, *Acta Crystallogr.*, 2008, **A64**, 112.
- G. M. Sheldrick, *SADABS, Program for Empirical Absorption Correction*, University of Göttingen, Göttingen, Germany, 1996.

- 31 M. J. Frisch, G. W. Trucks, H. B. Schlegel, G. E. Scuseria, M. A. Robb, J. R. Cheeseman, G. Scalmani, V. Barone, B. Mennucci, G. A. Petersson, H. Nakatsuji, M. Caricato, X. Li, H. P. Hratchian, A. F. Izmaylov, J. Bloino, G. Zheng, J. L. Sonnenberg, M. Hada, M. Ehara, K. Toyota, R. Fukuda, J. Hasegawa, M. Ishida, T. Nakajima, Y. Honda, O. Kitao, H. Nakai, T. Vreven, J. A. Montgomery Jr, J. E. Peralta, F. Ogliaro, M. Bearpark, J. J. Heyd, E. Brothers, K. N. Kudin, V. N. Staroverov, T. Keith, R. Kobayashi, J. Normand, K. Raghavachari, A. Rendell, J. C. Burant, S. S. Iyengar, J. Tomasi, M. Cossi, N. Rega, J. M. Millam, M. Klene, J. E. Knox, J. B. Cross, V. Bakken, C. Adamo, J. Jaramillo, R. Gomperts, R. E. Stratmann, O. Yazyev, A. J. Austin, R. Cammi, C. Pomelli, J. W. Ochterski, R. L. Martin, K. Morokuma, V. G. Zakrzewski, G. A. Voth, P. Salvador, J. J. Dannenberg, S. Dapprich, A. D. Daniels, O. Farkas, J. B. Foresman, J. V. Ortiz, J. Cioslowski, and D. J. Fox, Gaussian 09, Revision D.01, Gaussian, Inc., Wallingford CT, 2013.
- 32 W. J. Hehre, L. Radom, P. v.R. Schleyer and J. A. Pople, *Ab Initio Molecular Orbital Theory*, John Wiley & Sons, NY, 1986.
- 33 R. G. Parr and W. Yang, in *Density Functional Theory of Atoms and Molecules*; Oxford University Press: New York, 1989.
- 34 (a) J. P. Perdew, K. Burke and M. Ernzerhof, *Phys. Rev. Lett.*, 1997, **78**, 1396; (b) J. P. Perdew, *Phys. Rev. B*, 1986, **33**, 8822.
- 35 (a) U. Haeusermann, M. Dolg, H. Stoll and H. Preuss, *Mol. Phys.*, 1993, **78**, 1211; (b) W. Kuechle, M. Dolg, H. Stoll and H. Preuss, *J. Chem. Phys.*, 1994, **100**, 7535; (c) T. Leininger, A. Nicklass, H. Stoll, M. Dolg and P. Schwerdtfeger, *J. Chem. Phys.*, 1996, **105**, 1052.
- 36 A. W. Ehlers, M. Böhme, S. Dapprich, A. Gobbi, A. Höllwarth, V. Jonas, K. F. Köhler, R. Stegmann, A. Veldkamp and G. Frenking, *Chem. Phys. Lett.*, 1993, **208**, 111.
- 37 (a) A. D. McLean and G. S. Chandler, *J. Chem. Phys.*, 1980, **72**, 5639; (b) R. Krishnan, J. S. Binkley, R. Seeger and J. A. Pople, *J. Chem. Phys.*, 1980, **72**, 650; (c) A. J. H. Wachters, *J. Chem. Phys.*, 1970, **52**, 1033; (d) P. J. Hay, *J. Chem. Phys.*, 1977, **66**, 4377; (e) K. Raghavachari and G. W. Trucks, *J. Chem. Phys.*, 1989, **91**, 1062; (f) R. C. Binning Jr. and L. A. Curtiss, *J. Comp. Chem.*, 1990, **11**, 1206; (g) M. P. McGrath and L. Radom, *J. Chem. Phys.*, 1991, **94**, 511.
- 38 (a) C. Peng, P. Y. Ayala, H. B. Schlegel and M. J. Frisch, *J. Comp. Chem.*, 1996, **17**, 49; (b) C. Peng and H. B. Schlegel, *Israel J. Chem.*, 1993, **33**, 449.
- 39 (a) T. Clark, J. Chandrasekhar, G. W. Spitznagel and P. v. R. Schleyer, *J. Comp. Chem.*, 1983, **4**, 294; (b) M. J. Frisch, J. A. Pople and J. S. Binkley, *J. Chem. Phys.*, 1984, **80**, 3265.
- 40 Y. Zhao and D. G. Truhlar, *Theor. Chem. Acc.*, 2008, **120**, 215.
- 41 (a) Y. Zhao and D. G. Truhlar, *Acc. Chem. Res.*, 2008, **41**, 157; (b) Y. Zhao and D. G. Truhlar, *Chem. Phys. Lett.*, 2011, **502**, 1.
- 42 (a) M. T. Cancès, B. Mennucci and J. Tomasi, *J. Chem. Phys.*, 1997, **107**, 3032; (b) M. Cossi, V. Barone, B. Mennucci and J. Tomasi, *Chem. Phys. Lett.*, 1998, **286**, 253; (c) B. Mennucci and J. Tomasi, *J. Chem. Phys.*, 1997, **106**, 5151; (d) J. Tomasi, B. Mennucci and R. Cammi, *Chem. Rev.*, 2005, **105**, 2999.
- 43 A. V. Marenich, C. J. Cramer and D. G. Truhlar, *J. Phys. Chem. B*, 2009, **113**, 6378.
- 44 <https://www.chemcraftprog.com>.